Ceramic Tubular MOF Hybrid Membrane Fabricated through *In Situ* Layer-by-Layer Self-Assembly for Nanofiltration

Naixin Wang, Tianjiao Liu, Hongpan Shen, Shulan Ji, and Jian-Rong Li
Beijing Key Laboratory for Green Catalysis and Separation, College of Environmental and Energy Engineering, Beijing University of Technology, Beijing 100124, P.R. China

Rong Zhang
Division of Nuclear Materials and Fuel, State Nuclear Power Research Institute, Beijing 100029, P. R. China

Beijing Key Laboratory for Green Catalysis and Separation, College of Environmental and Energy Engineering, Beijing University of Technology, Beijing 100124, P.R. China

DOI 10.1002/aic.15115
Published online December 8, 2015 in Wiley Online Library (wileyonlinelibrary.com)

Nanofiltration has been playing an important role in water purification, in which the developments of novel membrane materials and modules are among significant. Herein, a metal-organic framework (MOFs) hybrid membrane, ZIF-8/PSS was fabricated on a tubular alumina substrate through a layer-by-layer self-assembly technique. ZIF-8 particles in situ grow into PSS layers to improve their compatibility and dispersion, thereby getting high quality membrane, which was loaded into a steel tubular module for nano-filtrating dyes from water. Under optimized conditions, it shows outstanding nanofiltration properties toward methyl blue, with the flux of 210 Lm^{-2} h^{-1} MPa^{-1} and the rejection of 98.6%. Furthermore, the good pressure resistance ability and running stability of the membrane were revealed, which can be attributed to use the ceramic substrate and the inherent stability of ZIF-8. This work thus illustrates a simple approach for fabricating MOFs hybrid membranes on tubular ceramic substrates, having great potential for industrial applications. © 2015 American Institute of Chemical Engineers *AIChE J*, 62: 538–546, 2016

Keywords: in situ self-assembly, layer-by-layer fabrication, metal-organic framework hybrid membrane, tubular ceramic substrate, nanofiltration

Introduction

Nanofiltration is a pressure-driven membrane separation process, with a molecular weight cutoff (MWCO) range from 100 to 1000. Compared with reverse osmosis (RO), nanofiltration has the advantages of high flux, low operation pressure, and low-energy consumption.[1] It has been widely used in some fields, such as water purification, water softening, and desalination.[2] Among them, the retention and concentration of dyes from water are one of the largest applications for nanofiltration.[3] The crucial concern for its application in industry includes reducing membrane fouling, increasing membrane separation performance, and improving membrane lifetime and stability.[4] Developing new membrane material and exploring facile membrane preparation technique are effective ways to solve these problems.

Commercial nanofiltration membranes are mainly prepared by organic polymers, including cellulose acetate, polyamide, sulfonated polyethersulfone, sulfonated polysulfone, polyvinyl alcohol, polyphenylene oxide, polyethylenimine, and so on.[5] Although these membranes show good rejection toward large molecules, the permeances are still unsatisfactory for the real application. To improve the membrane permeability, various nanoparticles have been incorporated into the polymer to prepare hybrid membranes.[2,5] Simultaneously, the mechanical properties and stability of the membranes can be improved through the nanoparticles incorporation in some cases. Explored nanoparticles in nanofiltration membrane fabrication include metal oxides,[6] silica,[7] graphene oxide,[8] and metal-organic frameworks (MOFs).[9] Among them, MOFs, as a kind of newly developed porous materials are attracting intense interest. MOFs are built by organic linkers and metal nodes, which endow with better compatibility with the polymer in forming a hybrid membrane. Moreover, the pore size/shape, surface properties, and particle size of MOFs can be easily tuned to suit the requirements for the membrane fabrication and specific separations.[10,11] Recently, some MOF-based membranes have been used in nanofiltration. For example, Cohen et al.[12] prepared a series of MOF-polymer hybrid membranes with different MOFs including UiO-66, MIL-101(Cr), MIL-101(Fe), HKUST-1, MIL-53(Fe), and ZIF-8 on different substrates. These membranes showed good performances in the nanofiltration separation of dyes from water. Livingston et al.[13] used ZIF-8, MIL-53(Al), NH_2-MIL-53(Al), and MIL-101(Cr) to fabricate MOF hybrid membranes in a polyamide

Additional Supporting Information may be found in the online version of this article.

Correspondence concerning this article should be addressed to J.-R. Li at jrli@bjut.edu.cn.

(PA) thin film layer. The resulting membrane represented good performances in the organic solvent nanofiltration. It was found that the permeance of the membranes increased with increasing pore size of the used MOFs.

Besides membrane materials, the separation behavior of hybrid membranes was also affected by their structures, which can be regulated and controlled by the fabrication process. Usually used preparation methods for nanofiltration membranes include interfacial polymerization, grafting polymerization, and layer-by-layer (LbL) assembly. Among them, the interfacial polymerization is much more popular and widely used in preparing most commercial nanofiltration membranes.[14,15] Recently, a ZIF-8 hybrid membrane was fabricated on polyethersulfone (PES) substrate by an interfacial synthesis method, being similar to the interfacial polymerization.[9] This membrane was used for the dye retention from water and organic solvent. When the membrane prepared with 22% polymer concentration, the Rose Bengal (RB) rejection for ZIF-8/PES membrane significantly improved from 38.2 to 98.9%, with the permeance decreased from 277 to 13 $kgm^{-2}\ h^{-1}\ MPa^{-1}$. The ZIF-8/PES membrane showed a relatively high rejection, but the flux should be further improved to meet the requirements of industrial application. In our pervious study, using the LbL method a ZIF-8/PSS (PSS = poly(sodium 4-styrenesulfonate)) hybrid membrane was fabricated on a polyacrylonitrile (PAN) substrate by the *in situ* self-assembly strategy.[16] In this preparation process, ZIF-8 particles are simultaneously generated in the polymer during the formation of the membrane, thus resulting in their good dispersion. And, due to the coordination interactions between metal ions and the functional groups of the polymer, the resulting membrane represented improved MOF particle compatibility with the polymer and high stability, thereby excellent performances in the separation of dyes from water.

It should be emphasized that compared with the polymer substrates, ceramic substrates have advantages of high-temperature tolerance, well mechanical strength, and good antiswelling properties.[17,18] Furthermore, tubular membrane modules were shown to be more effective than flat-sheet arrangements for separation applications, because of their higher packing density.[19,20] Therefore, tubular ceramic membranes will have bright application prospects. Unfortunately, the related studies for the nanofiltration membrane fabrication using tubular ceramic substrate are lacking, with only two examples being reported by our group.[18,21]

In this work, ZIF-8/PSS hybrid membrane was fabricated by the *in situ* LbL self-assembly method on tubular ceramic substrate and used in dye (methyl blue, MB) nanofiltration from water. By this fabrication method, the compatibility and dispersion of ZIF-8 particles with/in PSS are greatly enhanced, which finally leads to high stability and excellent nanofiltration performances of the resulting membrane. In addition, the obtained hybrid membrane shows good mechanical strength due to the use of the ceramic substrate. The resulting membranes thus have a great potential in the practical applications of water purification through nanofiltration. This work also further promotes the research progress for using ceramic tubular membranes in nanofiltration field.

Experimental Section

Materials

Ceramic tubular substrates of 100 mm long and 8.5 mm inner and 13.5 mm outer diameters were obtained from JieXi LiShun Technology, China. The substrate is composed of the support layer (α-Al_2O_3) and the dense layer (γ-Al_2O_3). The γ-Al_2O_3 layer is on the outer surface of the substrate. 3-Aminopropyl-trimethoxysilane (APTES, Mw is 179.29), Poly(sodium 4-styrenesulfonate) (PSS, average Mw is 10,000,00), $Zn(NO_3)_2{\cdot}6H_2O$, and 2-methylimidazole (Hmim) were purchased from Sigma-Aldrich. Methanol and methyl blue (MB) were provided by Beijing Chemical Factory. The structure of methyl blue molecule is shown in Supporting Information Figure S1 and its dimension is provided in Supporting Information Table S1. All chemicals were used as received without further purification.

Preparation of ceramic tubular ZIF-8/PSS hybrid membrane

The ceramic tubular substrate was pretreated with the method reported by us.[22,23] It was immersed in a mixture of 95 wt% ethanol aqueous solution and 8 g L^{-1} 3-aminopropyl-trimethoxysilane aqueous solution for 2 h. Then, the substrate was rinsed by deionized water and dried in an oven at 110°C for 2 h.

The preparation of ZIF-8/PSS membrane on a grafted ceramic substrate was conducted using an LbL assembly method. The pretreated ceramic substrate was first immersed into 0.3 wt% PSS aqueous solutions for 30 min at 60°C. Then the substrate was rinsed by deionized water and dried in an oven at 60°C for 1 h. The PSS-grafted ceramic substrate was then immersed in $Zn(NO_3)_2$ methanol solution for 30 min at 60°C, followed by methanol rinsing for 10 min. Then the substrate was dried in an oven at 60°C for 1 h. After that, the ceramic substrate was immersed in the mixture of Hmim methanol solution ($C_{Zn(NO3)2} : C_{Hmim} = 1{:}4$) and 0.3 wt% PSS aqueous solution ($V_{PSS} : V_{Hmim} = 1{:}1$) at 60°C for 1 h. Finally, the resulting ceramic tubular hybrid membrane was rinsed by methanol for 10 min and dried in an oven at 60°C for 1 h. Using this method, $Zn(NO_3)_2$ and PSS/Hmim were alternatively assembled onto the surface of the ceramic substrate. To generate multiple layer membrane, additional Zn^{2+} ions were assembled on the first layer of the membrane and then assemble with PSS/Hmim. This cycling process was repeated to obtain final membranes.

Nanofiltration experiments

As shown in Supporting Information Figure S3, dye removal experiment was performed using a cross flow nanofiltration system which contains membrane module, plunger pump, pressure gauge, and solution vessel. The membrane module was a four-channel steel tube (Supporting Information Figure S2).[18] The feed solution with a dye concentration of 100 mg/L was pressurized with a plunger pump. During the nanofiltration process, the concentrate was recirculated to the feed vessel while permeate was collected in permeate vessel.

The permeation flux J ($Lm^{-2}\ h^{-1}\ MPa^{-1}$) was calculated by

$$J = \frac{V}{At\Delta P} \tag{1}$$

V (L) was the amount of permeate collected under operating pressure P (MPa) on a time scale t (h) and A was the effective area of the membrane (m^2).

The solute rejection rate R was calculated by

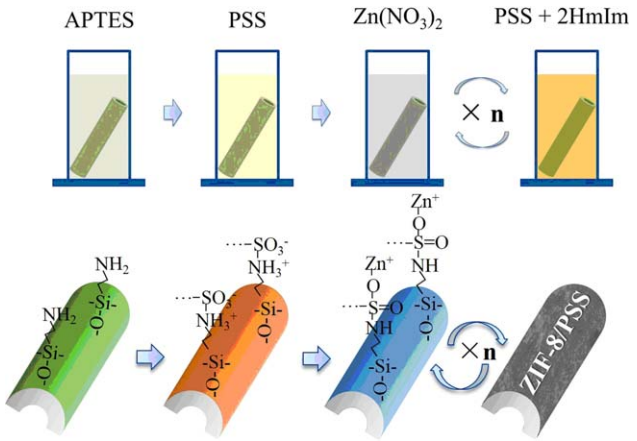

Figure 1. Schematic illustration of preparing ZIF-8/PSS membrane on a tubular ceramic substrate by a layer-by-layer assembly method.

[Color figure can be viewed in the online issue, which is available at wileyonlinelibrary.com.]

$$R(\%)=100\times\left(1-\frac{C_p}{C_f}\right) \tag{2}$$

The C_p and C_f represent the solute concentration of permeate and feed solutions, respectively. The dye concentrations were measured by an ultraviolet-visible spectrophotometer (UV2800, Shanghai) at the maximal absorption wavelength of the dye.

Characterizations

The surface and cross-section morphologies of the membranes were observed by field emission scanning electron microscopy (SEM) (Model SU-8020, Hitachi, Japan) and atomic force microscope (AFM) (Pico Scan TM 2500). An energy dispersive X-ray (EDX) unit was used for the determination of the elemental components of the membranes. All membranes were dried under a vacuum. Powder X-ray diffraction (PXRD) patterns were collected on a Bruker AXS D8 Advance diffractometer using Cu-*K*a radiation. The Young's modulus and hardness of the hybrid membranes were characterized by a Nano Indenter G200 (Agilent Technology).

Results and Discussion

As shown in Figure 1, the ZIF-8/PSS hybrid membrane was prepared by the *in situ* LbL self-assembly method on the tubular ceramic substrate. The ceramic tube was first pretreated by silane coupling agents before the membrane assembly to improve the adhesion with hereafter forming ZIF-8/PSS membrane. Then, it is expected that the amino group ($-NH_2$) in silane coupling agents can combine with the sulfonic acid group ($-SO_3H$) in PSS through the electrostatic interaction/acid-base reaction. After that, the $Zn(NO_3)_2$ and PSS/Hmim mixtures were alternatively assembled onto the functionalized ceramic tube by the coordination-driven *in situ* self-assembly strategy developed by us.[16] It should be pointed out that during the formation of the hybrid membrane Zn^{2+} ions could simultaneously coordinate with PSS and mim, which leads to that formed ZIF-8 particles *in situ* generate into PSS with high dispersion and form strong interaction with the polymer. To generate multiple layers, an LbL method was adopted, in which additional Zn^{2+} ions were assembled on the first layer of the membrane through the coordination with the sulfonate groups of PSS and then reaction with PSS and mim to form an additional membrane layer. This cycling process was repeated until the desired membrane was achieved.

To determine the formation of crystalline ZIF-8 particles inside the PSS membrane, PXRD was used to characterize the ceramic tube and ZIF-8/PSS hybrid membrane. As shown in Figure 2, the simulated ZIF-8 crystals have several characteristic peaks from 5° to 30° (Figure 2a), while characteristic peaks of the ceramic tube are in the range of 25–60° (Figure 2b). It is clear that the peaks of ceramic ZIF-8/PSS membrane match well with the pure ZIF-8 crystals and the ceramic substrate (Figure 2c). The formation of ZIF-8 crystals in PSS membrane can thus be confirmed.

As shown in Supporting Information Figure S4a, the tubular substrate is composed of the support layer and the dense layer. The dense layer is on the outer surface of the substrate, with the thickness of approximately 5 μm and the pore size of about 100 nm (Figure 3a and Supporting Information S4b). For checking the membrane formation on the ceramic tubular substrate, the surface morphologies of the dense layer before and after membrane assembly were characterized by SEM. As shown in Figures 3b–d, after the assembly of ZIF-8/PSS membrane, the outer surface of the ceramic substrate was clearly covered. Subsequently, with the layer numbers increased from two layers to six layers, the ZIF-8 particles grew together and the ZIF-8/PSS membrane became increasingly denser. In addition, the polyhedral shape of ZIF-8 particles, which are wrapped by PSS chains with good compatibility, can be identified clearly on the membrane surface. It should be pointed out that during assembling the membrane, the precursor concentration of forming the MOF also has an important influence on the structure of the resulting membrane. The surface morphology of ZIF-8/PSS membrane prepared under different $Zn(NO_3)_2$ concentrations are shown in Figures 3c, e, f. It was found that with the $Zn(NO_3)_2$ concentration increased from 0.05 to 0.4 mol L^{-1}, the resultant ZIF-8/PSS membrane became more and more dense, which can be explained as that the particle size of ZIF-8 decreased as the $Zn(NO_3)_2$ concentration increased, while the amount of the particles increased.

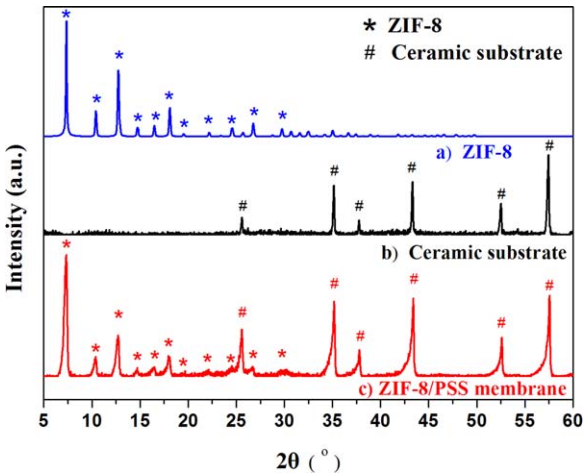

Figure 2. PXRD patterns of (a) simulated ZIF-8 crystals, (b) pure ceramic tubular substrate, and (c) ZIF-8/PSS membrane on the ceramic substrate.

[Color figure can be viewed in the online issue, which is available at wileyonlinelibrary.com.]

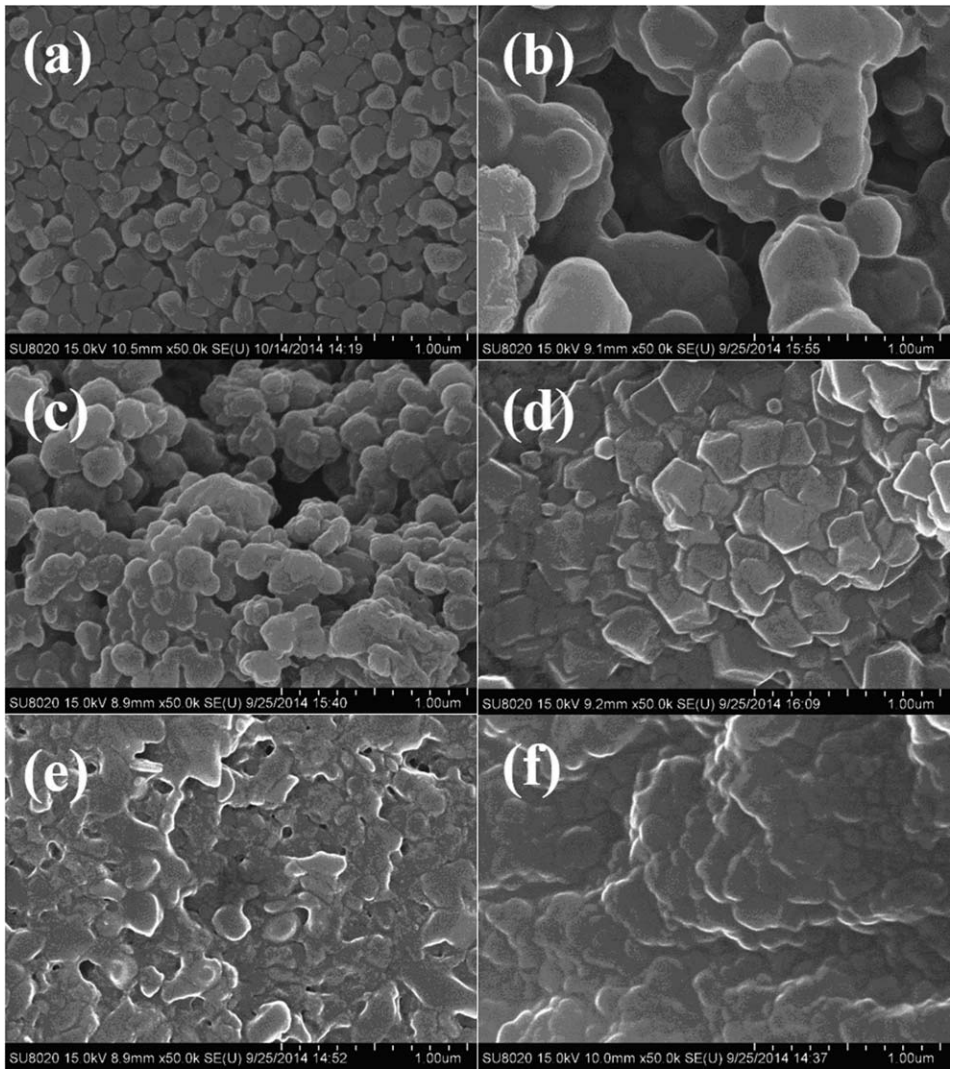

Figure 3. SEM images of surface morphologies of the ceramic substrate (a) and the ZIF-8/PSS hybrid membrane with two layers (b), four layers (c), and six layers (d) (×50 k) (preparation condition: $C_{Zn(NO_3)2} = 0.05$ mol L^{-1}); as well as the ZIF-8/PSS membranes prepared under different $Zn(NO_3)_2$ concentrations of 0.2 mol L^{-1} (e), and 0.4 mol L^{-1} (f) (×50 k) (preparation condition: four assembly layers).

It results in smaller ZIF-8 particles growing together to make the membrane much more compact. Moreover, comparing the inner surface of ceramic substrate before (Supporting Information Figure S4c) and after (Supporting Information Figure S4d) assembly, it can be found that the morphologies of the ceramic inner surface have no obvious change. Therefore, ZIF-8/PSS active layer was only formed on the outer surface of the tubular substrate.

In addition, the surface microstructure of the ceramic substrate and ZIF-8/PSS hybrid membranes prepared under different conditions were also characterized by AFM. As shown in Figure 4a, the root mean square roughness of the ceramic substrate was evaluated to be 55.9 nm, and the ceramic particles can be seen on the surface. When the substrate was covered by the ZIF-8/PSS membrane with four assembly layers (0.05 mol L^{-1} $Zn(NO_3)_2$ as the precursor), the roughness of the membrane surface increased to 145 nm (Figure 4b) due to the existence of the ZIF-8 particles on the membrane surface. Conversely, a morphology with regular texture structure was observed on the surface of ZIF-8/PSS membrane, being totally different from that of a ZIF-8/PSS membrane assembled on polymer substrate.[16] Another interest finding is that the growth of ZIF-8 crystals on the ceramic substrate is orientated, which makes the ZIF-8/PSS membrane shows a self-modification ability with the sustained growth of ZIF-8 crystals. Therefore, when the assembly layer increased to six layers (Figure 4c), the roughness of membrane surface decreased to 107 nm, being consistent with the observation of SEM images. In addition, the effect of $Zn(NO_3)_2$ concentration on the membrane microstructure was also investigated. It was found that when the $Zn(NO_3)_2$ concentration increased from 0.05 to 0.2 mol L^{-1}, the roughness of the membrane surface increased from 145 to 245 nm. The possible reason may be that the ZIF-8/PSS membrane, which prepared from high $Zn(NO_3)_2$ concentration, has smaller particles in the membrane.

The layer organization of the whole membrane and the thickness of the ZIF-8/PSS layer were identified based on the cross-section morphology observation. As shown in Figures 5a, b, the ZIF-8/PSS hybrid membrane shows an obvious three layer structure, including ZIF-8/PSS layer, ceramic dense layer, and ceramic support layer. It is clear that from the SEM images the ZIF-8/PSS thin film with a thickness of 5 μm was

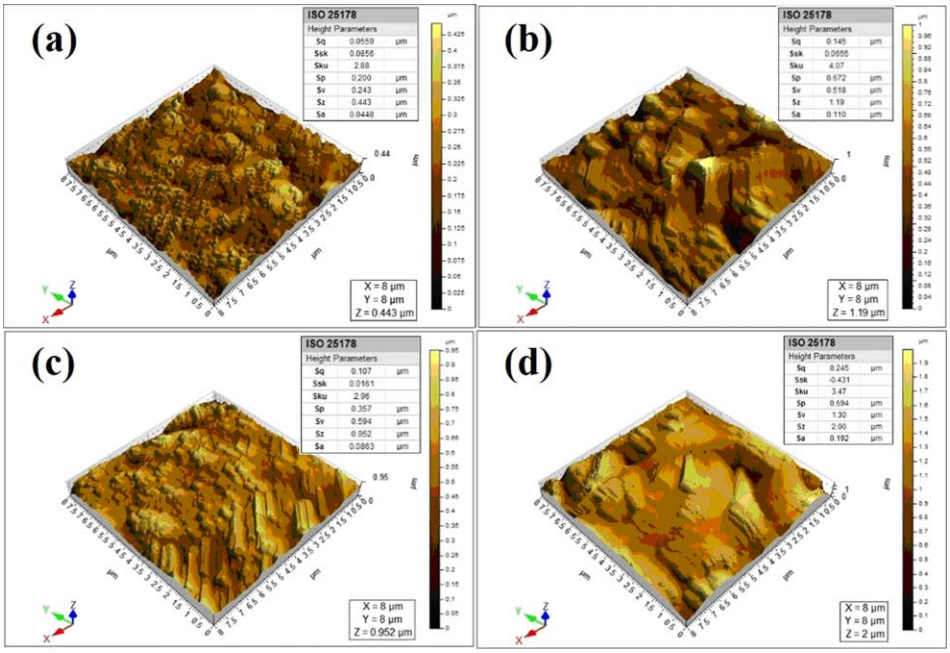

Figure 4. AFM images of tubular ceramic substrate (a) and ZIF-8/PSS hybrid membranes with 0.05 mol L^{-1} $Zn(NO_3)_2$ and four layers (b), 0.05 mol/L $Zn(NO_3)_2$ and six layers (c), and 0.2 mol L^{-} $Zn(NO_3)_2$ and four layers (d).

[Color figure can be viewed in the online issue, which is available at wileyonlinelibrary.com.]

assembled on the surface of the ceramic dense layer. To further analyze the microstructure and check the elemental distribution of the ZIF-8/PSS layer, elemental mapping was reported by EDX measurements on the cross-section of the membrane. The corresponding elemental mapping images of aluminum, zinc, oxygen, and carbon are shown in Figures 5c–f, from which a clear interface between the ZIF-8/PSS layer and the ceramic dense layer was observed. It was also found that a small amount of zinc element exists in the ceramic dense layer, suggesting that ZIF-8/PSS might filtrate into the pores of the ceramic substrate. That is, ZIF-8/PSS penetrates into the pores of ceramic support, rather than merely adsorbing onto the surface of the substrate. As a result, the ZIF-8/PSS layer combines well with the ceramic substrate to make the separation layer hardly peel off from the substrate, resulting in a robust hybrid membrane.

Furthermore, the mechanical properties of the ZIF-8/PSS hybrid membrane were determined by a Nano Indenter with nanoindentation. The Young's modulus and hardness were obtained by analyzing the changes of harmonic continuous stiffness on the membrane surface. The data were collected from randomly selected 20 points on the membrane surface and the average values are shown in Supporting Information Figure S5. An interesting phenomenon was observed that both Young's modulus and hardness of ZIF-8/PSS hybrid membrane represent two numerical ranges. Based on the data analysis corresponding two ranges can be regarded a soft segment (polymer) and a hard segment (particle), resulting from PSS and ZIF-8 in the hybrid membrane, respectively. In the initial 50 nm, the error is clearly large due to the rough membrane surface. With the displacement into surface increased from 50 to 150 nm, the Young's modulus and hardness decreased sharply. However, these values changed to be steady when the displacement into the surface increased from 150 to 400 nm. The average values of the plateau range were thus used as the Young's modulus and hardness of the hybrid membrane. When the displacement into surface further increased, the Young's modulus and hardness were affected by the ceramic substrate. In addition, the Young's modulus and hardness of ZIF-8/PSS hybrid membranes with different thickness (layers) were also investigated. As shown in Supporting Information Figure S5c, d, when the assembly layer increased from four to six layers, the mechanical properties of the ZIF-8/PSS hybrid membrane improved obviously, a result of more ZIF-8 particles being assembled on the membrane surface. It was also found that the $Zn(NO_3)_2$ concentration has a significant effect on the mechanical properties of the ZIF-8/PSS hybrid membrane. When the $Zn(NO_3)_2$ concentration increased from 0.05 to 0.2 mol L^{-1}, both the Young's modulus and hardness of the hybrid membrane increased. This is because that the high concentration of the precursor can produce more ZIF-8 particles in the hybrid membrane, which enhance the mechanical property of the membrane resulting of the inorganic components in ZIF-8 particles.

The tubular ceramic ZIF-8/PSS hybrid membranes were thus used for removing dye (methyl blue, MB) from water by nanofiltration. As we know, for a multilayer membrane, the layer number has a great influence on its separation behavior. The nanofiltration performances of the hybrid membranes with different numbers of ZIF-8/PSS layers are shown in Figure 6. It was found that the rejection and flux of original ceramic support were 30.4% and 866 Lm^{-2} h^{-1} MPa^{-1}, respectively. Clearly, the separation performance of the ceramic substrate for dye removal is bad. When the substrate was assembled by one layer of ZIF-8/PSS, the nanofiltration ability was greatly improved with the rejection up to 85.3%. Increasing the number of ZIF-8/PSS layers leads to an increase of the dye rejection, while the flux decreased clearly. Such as, the rejection was 94.0% for a two layers ZIF-8/PSS membrane, but reached 99.4% for a seven layers one.

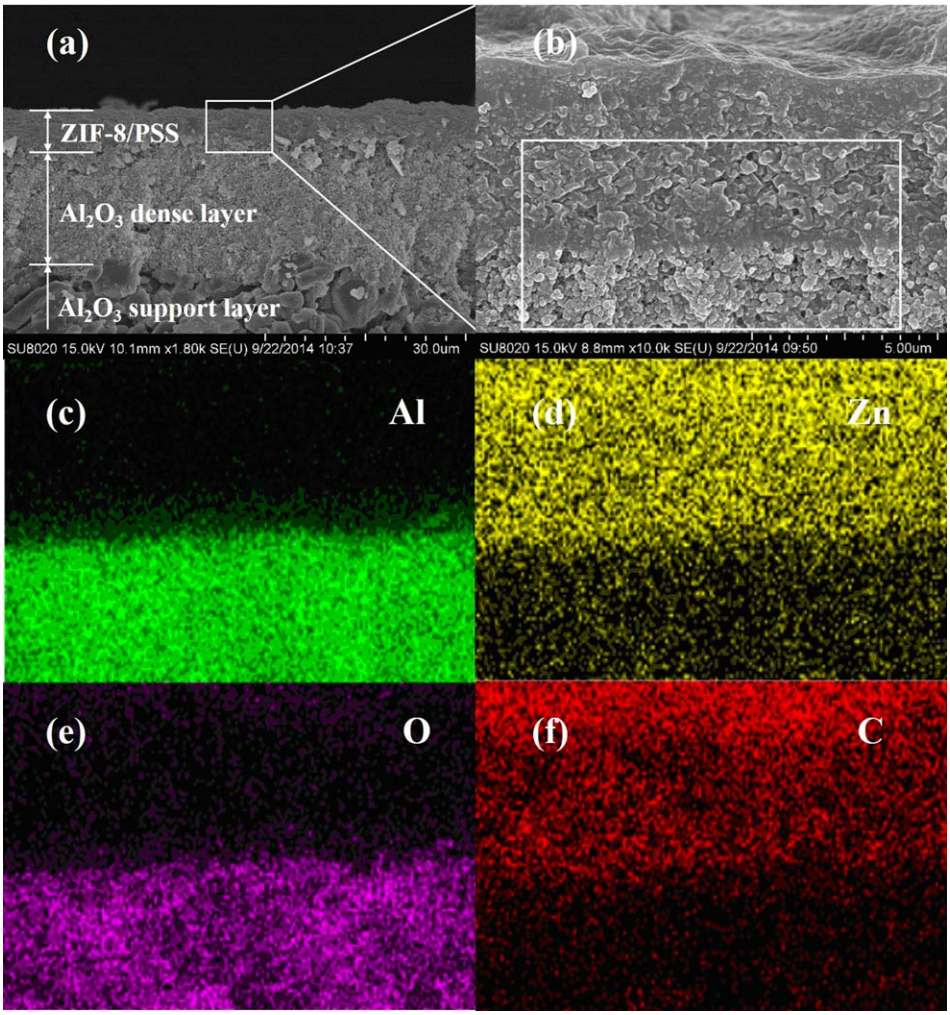

Figure 5. SEM images of (a) cross-section morphology of the ZIF-8/PSS membrane on the ceramic substrate (×1.8 k); (b) magnified cross-section morphology of the ZIF-8/PSS membrane (×50 k); and the elemental mapping images of aluminum (c), zinc (d), oxygen (e), and carbon (f) (Al in green, Zn in yellow, O in violet, and C in red; preparation conditions: $C_{Zn(NO_3)2} = 0.4$ mol L^{-1}; four assembly layers).

[Color figure can be viewed in the online issue, which is available at wileyonlinelibrary.com.]

Simultaneously, the flux decreased from 291 to 92 Lm^{-2} h^{-1} MPa^{-1}. This can be explained as that the membrane became denser and more compact with increasing ZIF-8/PSS layers. Considering the comprehensive performance including both rejection and flux, the membrane prepared with four layers with the rejection and flux of 97.4% and 230 Lm^{-2} h^{-1}

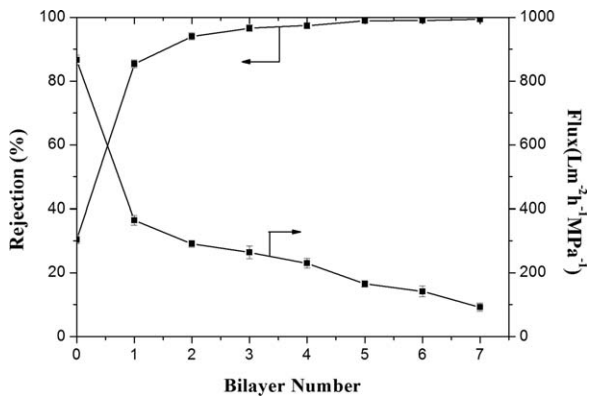

Figure 6. Effect of layer numbers on the nanofiltration performances of the ZIF-8/PSS membranes (preparation condition: $C_{Zn(NO_3)2} = 0.05$ mol L^{-1}).

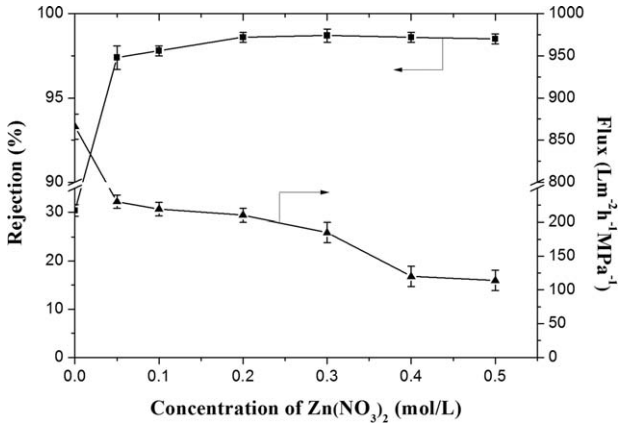

Figure 7. Effect of $Zn(NO_3)_2$ concentration on the nanofiltration performances (Preparation condition: four assembly layers).

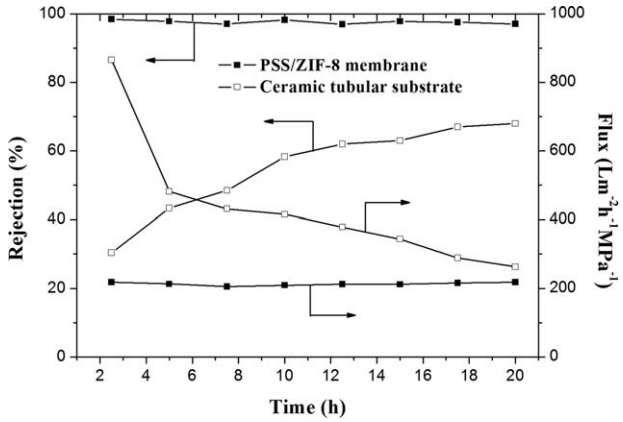

Figure 8. Stability tests of the ZIF-8/PSS hybrid membrane and the ceramic tubular substrate (preparation conditions: $C_{Zn(NO_3)2} = 0.2$ mol L^{-1}, four assembly layers; operating conditions: 0.5 MPa, 100 mg L^{-1} methyl blue aqueous solution).

MPa^{-1}, respectively, was suggested having an optimal separation performance. Therefore, four layers were selected as the best assembly condition in the following study.

Supposedly, the amount of ZIF-8 particles dispersed in PSS should have an important effect on the membrane performances. In this study, the amount of ZIF-8 particles was tuned by changing the concentration of the precursors, $Zn(NO_3)_2$ and Hmim, during the LbL self-assembly process. Because of the ratio of $Zn(NO_3)_2$ and Hmim was fixed at 1:4, the effect of the concentration of the ZIF-8 was explored in terms of the $Zn(NO_3)_2$ concentration. As shown in Figure 7, it was noted that the flux decreased from 230 to 114 Lm^{-2} h^{-1} MPa^{-1} as the $Zn(NO_3)_2$ concentration increased from 0.05 to 0.5 mol L^{-1}, while the rejection increased from 97.4 to 98.6%. Meanwhile, the particle size of ZIF-8 became smaller at high precursor concentration as discussed above. This result demonstrated that the increase of the small ZIF-8 particles in PSS can lead to the permeance decline and rejection increase toward MB of the resulting membrane. Considering both the rejection and flux, a $Zn(NO_3)_2$ concentration of 0.2 mol L^{-1} was chosen as the optimized condition for preparing following checked membrane. The separation performance of ZIF-8/PSS membrane could also be affected by the PSS concentration. As shown in Supporting Information Figure S6, with the PSS concentration increased from 0.1 to 0.3%, the rejection increased and the flux decreased. The improvement of separation performance could be due to such a fact that the ZIF-8 particles were wrapped by PSS chains much better with a higher PSS concentration than that on the lower concentration. The prepared membrane was thus much denser. However, when the PSS concentration increased from 0.3 to 0.6% both the rejection and the flux decreased. It is speculated that the excessive concentration of PSS causes the shrink of the PSS chains. The ZIF-8 particles can thus not be wrapped completely. Therefore, the tiny cracks between the particles might decrease the rejection. Moreover, high PSS concentration can increase the thickness of the separation layer, which leads to the increase in the mass-transfer resistance for water molecule, to make the flux reduce. Therefore, in the following research, 0.3% was chosen as the optimal concentration for PSS to assemble the ZIF-8/PSS multilayer membranes.

The effect of operation pressure on the MB removal performances of the optimized ZIF-8/PSS hybrid membrane was also investigated. As shown in Supporting Information Figure S7, the rejection and flux have no obvious change as the operation pressure increased from 0.2 to 0.6 MPa. This result reveals that the capability of the ZIF-8/PSS hybrid membrane for the MB removal was stable under different operation pressures. That is, the hybrid membrane fabricated by assembling ZIF-8/PSS on the ceramic substrate has a superior pressure resistance due to its strong mechanical property, having great potential for practical applications. In addition, the stability of the membrane for continuous use was also checked. A filtration of 20 h for the MB retention was taken. As shown in Figure 8, the dye rejection and flux of the membrane were basically maintained at a constant level, demonstrating that the ceramic ZIF-8/PSS hybrid membrane has a good stability for dye removal from water.

For comparison, the dye removal performances in different membranes are summarized in Table 1. We can find that up to now most of the reported nanofiltration membranes use polymers as the substrates. Although the testing conditions are different, to some extent, the results in this manuscript have demonstrated that the nanofiltration performances of our

Table 1. Comparison of the Dye Removal Performances in Different Membranes

Membrane	Substrate	Dye Molecule	Rejectio (%)	Flux (Lm^{-2} h^{-1} MPa^{-1})	Pressure (MPa)	Reference
F127/PES	PES	Alcian blue	95.7	176.2	0.2	1
ZIF-8/PA	PSf	Congo red	99.98	22.6	3	5
(PEI-GO)/PAA/PVA/GA	PAN	Methyl blue	99.3	8.7	0.5	8
ZIF-8/PES	PES	Rose bengal	98.9	13	–	9
ZIF-8/PSS	PAN	Methyl blue	98.6	265	0.5	16
CMCNa/PP	PP	Methyl blue	99.75	8.25	0.8	24
PVDF/nanoclay/chitosan	PVDF	Methyl blue	75	500	0.1	25
PES-TA(M-60)	PE	Methyl Green	>99.9	37.2	0.5	26
PES-SPMA	PES	Reactive Dyes	>98	145	0.4	27
PVDF-SAN-60	PVDF	Congo Red	97.7	95	0.4	28
(NaSS-AC)/PS	PSf	Acid red	96	58	0.4	29
Tannic acid/TMC	PES	Orange GII	99.7	168	0.2	30
PSF-PEG	PSf	Acid blue	98	76	0.4	31
$(PSS/PAH)_7$	Ceramic	Glutamine	86.2	132	0.48	32
PAA/PVA/GA	Ceramic tube	Congo red	96	42	0.6	21
PDDA/PSS	Ceramic tube	Methyl blue	92	82.5	0.6	18
ZIF-8/PSS	Ceramic tube	Methyl blue	98.6	210	0.5	This study

PES, polyethersulfone; PSf, polysulfone; PAN, polyacrylonitrile; PP, polypropylene; PVDF, poly(vinylidene fluoride); PE, Polyester.

ceramic tubular ZIF-8/PSS hybrid membrane are excellent, being comparable with other membranes. Particularly, the flux of the membrane can reach 210 Lm^{-2} h^{-1} MPa^{-1}, being higher than most of the reported nanofiltration membranes, and the membrane has very good stability. The separation mechanism of nanofiltration usually includes molecular sieving and Donnan effect. In this study, ZIF-8/PSS separation layer was formed on the surface of ceramic substrate. The pore size of ZIF-8/PSS membrane was less than 2 nm, which can not be observed from our SEM images. However, the pore size of the membrane can be determined from the MWCO. The MWCO of ceramic substrate and ZIF-8/PSS membrane was investigated through the filter polyethylene glycol (PEG) molecules with different molecular weights. The results show that the MWCO of ceramic substrate was over 20,000, while the ZIF-8/PSS membrane was about 500–600. As the molecular weight of methyl blue is 799.8, it could be rejected by ZIF-8/PSS membrane through the sieving effect. Moreover, the pore size of ZIF-8 particles is 0.34 nm (determined from single-crystal diffraction data of ZIF-8 crystals), which is much smaller than the size of a methyl blue molecule and larger than the size of a water molecule (0.27 nm). Therefore, water molecule can pass through the ZIF-8/PSS membrane from the channels of ZIF-8 and other pores, while the methyl blue molecule could just penetrate the membrane from PSS section and the interface spaces of PSS and ZIF-8. In addition, PSS is an anionic polyelectrolyte which has the same charge property with the methyl blue. Thus, the methyl blue molecule can also be rejected through the charge repulsion effect.

Conclusions

In sum, a tubular ceramic ZIF-8/PSS hybrid membrane was successfully prepared through the *in situ* LbL self-assembly method. ZIF-8 particles *in situ* grow into PSS during the membrane formation, which results in their good compatibility and uniform dispersion within it. It was found that the membrane has excellent nanofiltration performances for the dye removal from water. Under optimized conditions the membrane represents a flux of 210 Lm^{-2} h^{-1} MPa^{-1} and rejection of 98.6% toward the MB nanofiltration from water. Furthermore, the mechanical stability of the hybrid membrane is enhanced through using the ceramic substrate. As a result, the hybrid membrane shows good pressure resistance ability and running stability. Combined with the advantages of the tubular module, this tubular ceramic ZIF-8/PSS hybrid membrane has a great potential for practical applications such as in the nanofiltration of dyes and other large molecules from water. Further explorations for the application in practice are in progress in our lab.

Acknowledgments

This work was financially supported by the National Natural Science Foundation of China (No. 21322601, 21271015, 21406006), the National High Technology Research and Development Program of China (No. 2015AA03A062).

Literature Cited

1. Zhang Y, Su Y, Chen W, Peng J, Dong Y, Jiang Z. A feasible post-treatment of drying and rewetting for preparation of high-flux pluronic F127/polyethersulfone nanofiltration membranes. *Ind Eng Chem Res*. 2011;50:4678–4685.
2. Mohammad AW, Teow YH, Ang WL, Chung YT, Oatley-Radcliffe DL, Hilal N. Nanofiltration membranes review: recent advances and future prospects. *Desalination*. 2015;356:226–254.
3. Huang J, Zhang K. The high flux poly (m-phenylene isophthalamide) nanofiltration membrane for dye purification and desalination. *Desalination*. 2011;282:19–26.
4. Bruggen BV, Mänttäri M, Nyström M. Drawbacks of applying nanofiltration and how to avoid them: a review. *Sep Purif Technol*. 2008; 63:251–263.
5. Wang L, Fang M, Liu J, He J, Deng L, Li J, Lei J. The influence of dispersed phases on polyamide/ZIF-8 nanofiltration membranes for dye removal from water. *RSC Adv*. 2015;5:50942–50954.
6. Hou J, Dong G, Ye Y, Chen V, Enzymatic degradation of bisphenol-A with immobilized laccase on TiO_2 sol-gel coated PVDF membrane. *J Memb Sci*. 2014;469:19–30.
7. Zhang H, Mao H, Wang J, Ding R, Du Z. Mineralization-inspired preparation of composite membranes with polyethyleneimine–nanoparticle hybrid active layer for solvent resistant nanofiltration. *J Memb Sci*. 2014;470:70–79.
8. Wang N, Ji S, Zhang G, Li J, Wang L. Self-assembly of graphene oxide and polyelectrolyte complex nanohybrid membranes for nanofiltration and pervaporation. *Chem Eng J*. 2012;213:318–329.
9. Li Y, Wee LH, Volodin A, Martensa JA, Vankelecom IFJ. Polymer supported ZIF-8 membranes prepared via an interfacial synthesis method. *Chem Commun*. 2015;51:918–920.
10. Zhou H-C, Long JR, Yaghi O. Introduction to metal-organic frameworks. *Chem Rev*. 2012;112:673–674.
11. Li J-R, Yu J, Lu W, Sun L-B, Sculley J, Balbuedna PB, Zhou H-C. Porous materials with pre-designed single-molecule traps for CO_2 selective adsorption. *Nat Commun*. 2013;4:1538.
12. Denny MS, Cohen SM. In situ modification of metal–organic frameworks in mixed-matrix membranes. *Angew Chem Int Ed*. 2015;54: 9029–9032.
13. Sorribas S, Gorgojo P, Téllez C, Coronas J, Livingston AG. High flux thin film nanocomposite membranes based on metal-organic frameworks for organic solvent nanofiltration. *J Am Chem Soc*. 2013;135:15201–15208.
14. Tsuru T, Sasaki S, Kamada T, Shintani T, Ohara T, Nagasawa H, Nishida K, Kanezashi M, Yoshioka T. Multilayered polyamide membranes by spray-assisted 2-step interfacial polymerization for increased performance of trimesoyl chloride (TMC)/m-phenylenediamine (MPD)-derived polyamide membranes. *J Memb Sci*. 2013; 446:504–512.
15. Seman M, Khayet M, Hilal N. Nanofiltration thin-film composite polyester polyethersulfone-based membranes prepared by interfacial polymerization. *J Memb Sci*. 2010;348:109–116.
16. Zhang R, Ji S, Wang N, Wang L, Zhang G, Li J-R. Coordination-driven in situ self-assembly strategy for the preparation of metal-organic framework hybrid membranes. *Angew Chem Int Ed*. 2014; 53:9775–9779.
17. Zhu Y, Xia S, Liu G, Jin W. Preparation of ceramic-supported poly(-vinyl alcohol)–chitosan composite membranes and their applications in pervaporation dehydration of organic/water mixtures. *J Memb Sci*. 2010;349:341–348.
18. Tang H, Ji S, Gong L, Guo H, Zhang G. Tubular ceramic-based multilayer separation membranes using spray layer-by-layer assembly. *Polym Chem*. 2013;4:5621–5628.
19. Wolff C, Beutel S, Scheper T. Tubular membrane bioreactors for biotechnological processes. *Appl Microbiol Biotechnol*. 2013;97: 929–937.
20. Wang N, Zhang G, Ji S, Fan Y. Dynamic layer-by-layer self-assembly of organic–inorganic composite hollow fiber membranes. *AIChE J*. 2012;58:3176–3182.
21. Wang L, Wang N, Zhang G, Ji S. Covalent crosslinked assembly of tubular ceramic-based multilayer nanofiltration membranes for dye desalination. *AIChE J*. 2013;59(10):3834–3842.
22. Wu T, Wang N, Li J, Wang L, Zhang W, Zhang G, Ji S. Tubular thermal crosslinked-PEBA/ceramic membrane for aromatic/aliphatic pervaporation. *J Memb Sci*. 2015;486:1–9.
23. Zhang Y, Wang N, Ji S, Zhang R, Zhao C, Li J-R. Metal-organic framework/poly(vinyl alcohol) nanohybrid membrane for the pervaporation of toluene/*n*-heptane mixtures. *J Memb Sci*. 2015;489:144–152.
24. Yu S, Chen Z, Cheng Q, Lü Z, Liu M, Gao C. Application of thin-film composite hollow fiber membrane to submerged nanofiltration of anionic dye aqueous solutions. *Sep Purif Technol*. 2012;88:121–129.
25. Daraei P, Madaeni SS, Salehi E, Ghaemi N, Ghari HS, Khadivi MA, Rostami E. Novel thin film composite membrane fabricated by mixed matrix nanoclay/chitosan on PVDF microfiltration support: preparation, characterization and performance in dye removal. *J Memb Sci*. 2013;436:97–108.

26. Zhang Q, Wang H, Zhang S, Dai L. Positively charged nanofiltration membrane based on cardo poly(arylene ether sulfone) with pendant tertiary amine groups. *J Memb Sci*. 2011;375:191–197.
27. Reddy AVR, Trivedi JJ, Devmuraru CV, Mohan DJ, Singh P, Rao AP, Joshi SV, Ghosh PK. Fouling resistant membranes in desalination and water recovery. *Desalination*. 2005;183:301–306.
28. Srivastava HP, Arthanareeswaran G, Anantharaman N, Starov VM. Performance of modified poly(vinylidene fluoride) membrane for textile wastewater ultrafiltration. *Desalination*. 2011;282:87–94.
29. Akbari A, Desclaux S, Rouch JC, Aptel P, Remigy JC. New UV-photografted nanofiltration membranes for the treatment of colored textile dye effluents. *J Memb Sci*. 2006;286:342–350.
30. Zhang Y, Su Y, Peng J, Zhao X, Liu J, Zhao J, Jiang Z. Composite nanofiltration membranes prepared by interfacial polymerization with natural material tannic acid and trimesoyl chloride. *J Memb Sci*. 2013;429:235–242.
31. Amini M, Arami M, Mahmoodi NM, Akbari A. Dye removal from colored textile wastewater using acrylic grafted nanomembrane. *Desalination*. 2011;267:107–113.
32. Hong SU, Bruening ML. Separation of amino acid mixtures using multilayer polyelectrolyte nanofiltration membranes. *J Memb Sci*. 2006;280:1–5.

Manuscript received July 31, 2015, and revision received Oct. 24, 2015.